Int. J. Rock Mech. Min. Sci. & Geomech. Abstr. Vol.30, No.7, pp. 1005–1008, 1993
Printed in Great Britain

0148-9062/93 $6.00 + 0.00
Pergamon Press Ltd

Gravitational Stresses in Long Asymmetric Ridges and Valleys in Anisotropic Rock

E. PAN†
B. AMADEI†

INTRODUCTION

When estimating the state of stress at any depth, z, in a rock mass due to gravity, it is commonly assumed that (1) the rock mass is an isotropic and linear elastic continuum, (2) the ground surface is horizontal, and (3) the state of stress is described by two principal stress components: a vertical component σ_v due to the weight of overlying rock at that depth and equal to γz and a horizontal component σ_h equal to K times σ_v. The simplifying assumption that the principal stresses are vertical and horizontal with depth breaks down when the ground surface is not horizontal. At the ground surface, the principal stresses must be parallel and normal to the topography in the absence of surface loads. With depth, the principal stresses turn and approach the same directions as when the ground surface is horizontal.

The effect of surface topography on gravitational stresses has been addressed in the past using two types of analytical methods. One is the exact conformal mapping method [1,2]. However, this approach is restricted to isotropic media, to a very few smooth topographic profiles for which conformal mapping functions can be found exactly, and to two dimensional problems. The other approach is to use the perturbation method [3-6]. The advantage of the perturbation method is that it can handle any smooth topographic features. However, the solutions derived with that method are restricted to topographies with small slopes less than 10%. All the solutions derived with the exact conformal mapping and perturbation methods show clearly that the topography can have a major effect on the magnitude and distribution of stresses in-situ.

In a recent paper, Pan and Amadei [7] presented a new analytical method for determining the stress field in a homogeneous, general anisotropic and elastic half space limited by irregular (but smooth) outer boundaries. The method is general enough in that the half space is subject to gravity and surface loads. Using the closed-form solutions of Amadei and Pan [8] and the analytical function method of Lekhnitskii [9], expressions for the stresses in an anisotropic half space with an irregular boundary were derived. The stresses were found to depend on three analytical functions that can be determined using a numerical conformal mapping method [10] and an integral equation method [11]. This solution was used more recently by the authors to determine gravity-induced stresses in long symmetric and transversely isotropic ridges and valleys with planes of anisotropy striking parallel to the ridge or valley axis [12]. A parametric study was presented on the effect of (1) topography shape and geometry, (2) orientation of anisotropy, and (3) degree of anisotropy on the magnitude and distribution of gravitational stresses.

This paper is an extension of the paper by Pan *et al.* [12]. A method is proposed to study the magnitude and distribution of gravitational stresses in transversely isotropic rock masses with asymmetric topographies. At the outset, it is shown how asymmetric topographies can be obtained by superposition of the topography of symmetric ridges and valleys. Then, the analytical formulation of Pan and Amadei [7] and Pan *et al.* [12] is modified to handle asymmetric topographies. Finally, numerical examples are presented showing how gravitational stresses in asymmetric ridges and valleys differ from those in symmetric and isolated topographies. Throughout this paper, it is assumed that the rock mass is transversely isotropic with planes of transverse isotropy parallel to the ridge or valley axis and deforms in plane strain.

FORMULATION FOR ASYMMETRIC TOPOGRAPHIES

Consider the equilibrium of a long asymmetric ridge with the geometry of Figure 1a. The half space represents a rock mass subject to gravity, g, only. The rock mass is linearly elastic, anisotropic, homogeneous and continuous

†Department of Civil Engineering, University of Colorado, Boulder, CO 80309-0428, U.S.A.

with a uniform density ρ. An x, y, z coordinate system is attached to the half space such that the x and z axes are in the horizontal plane and the y axis is pointing upward. The half space geometry and the rock mass elastic properties are assumed to be independent of the z direction. The boundary curve of the ridge is defined by a smooth function $y=y(x)$ or in parametric form

$$x(t)=t \qquad (-\infty<t<+\infty) \qquad (1)$$
$$y(t)=y_1(t)+y_2(t)$$

with

$$y_1(t)=\frac{a^2b}{(t-x_1)^2+a^2}; \qquad y_2(t)=\frac{c^2d}{(t-x_2)^2+c^2} \qquad (2)$$

In equation (2), b and d represent the heights of two ridges $x(t)$, $y_1(t)$ and $x(t)$, $y_2(t)$ centered at x_1 and x_2 ($x_1 \neq x_2$), respectively. Parameters a and c control the locations of the inflection points of each ridge. If b and d are negative, equations (1) and (2) correspond to an asymmetric valley consisting of two symmetric valleys with depths $|b|$ and $|d|$ and centered at x_1 and x_2 (Figure 1b). Other asymmetric topographies can be obtained by combining ridges and valleys with different positive and negative values of a, b, c, d, x_1 and x_2.

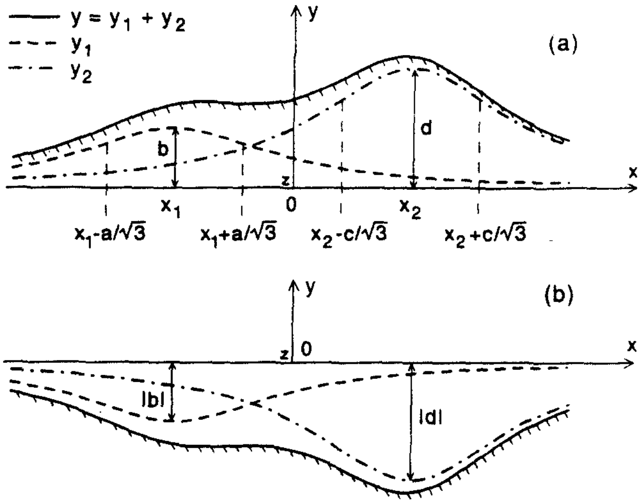

Figure 1. Asymmetric topographies obtained by superposition of two separate symmetric ridges and valleys (a) $b/|d|=0.5$ and $d/|d|=1$, (b) $b/|d|=-0.5$ and $d/|d|=-1$. In (a) and (b) $a/|d|=1$, $c/|d|=1$, $x_1/|d|=-1$, and $x_2/|d| = 1$.

As discussed previously by Pan and Amadei [7] and Pan *et al.* [12], determination of the gravitational stresses below a given smooth topography can be done by carrying out three successive conformal mappings. For the geometries of Figures 1a and 1b, the mappings are:

Mapping 1:

$$z_k \rightarrow w_k \qquad k=1,2 \qquad (3)$$
$$w_k(t)=\frac{x(t)+\mu_k y(t)+iA_k}{x(t)+\mu_k y(t)-iA_k} \qquad -\infty<t<\infty$$

maps the lower half planes bounded by $z_k = x(t) + \mu_k y(t)$ onto irregular bounded domains w_k. In equation (3), μ_k are complex numbers with positive imaginary parts and are the roots of equation (11) in [12]. A_k are complex constants chosen such that the mapping is conformal. As discussed in [12], the variable t in equation (3) can be replaced by a new parameter θ that varies over a finite interval $[-\pi/2, \pi/2]$ such that $t=\tan\theta$. Then, equation (3) takes the following form

$$w_k(\theta)=\frac{(\sin\theta+iA_k\cos\theta)/\mu_k+p_1(\theta)+q_1(\theta)}{(\sin\theta-iA_k\cos\theta)/\mu_k+p_1(\theta)+q_1(\theta)} \qquad (4)$$
$$k=1,2; \quad \frac{-\pi}{2}\leq\theta\leq\frac{\pi}{2}$$

with

$$p_1(\theta)=\frac{a^2b\cos^3\theta}{(\sin\theta-x_1\cos\theta)^2+a^2\cos^2\theta}$$

$$q_1(\theta)=\frac{c^2d\cos^3\theta}{(\sin\theta-x_2\cos\theta)^2+c^2\cos^2\theta}$$

Mapping 2:

$$w_k \rightarrow F_k \qquad k=1,2 \qquad (5)$$
$$F_k=F_k(w_k)$$

maps the irregular bounded domains w_k onto unit discs F_k. As discussed by Pan and Amadei, this is done using a numerical integral method [7,10].

Mapping 3:

$$F_k \rightarrow \zeta_k \qquad k=1,2 \qquad (6)$$
$$\zeta_k=i\frac{F_k(w_k)+1}{F_k(w_k)-1}$$

maps the unit discs F_k onto lower flat half-planes ζ_k.

For the topographies of Figures 1a and 1b, the functions $t'(t_j)$ and $t'_k(t_j)$ defined in equation (22) of [12] can be written as follows

$$t'(t_j)=\frac{Z_j'(t_j)}{1-2\mu_j r(t)} \quad ; \quad t_k'(t_j)=\frac{[1-2\mu_k r(t)]Z_j'(t_j)}{[1-2\mu_j r(t)]Z_k'(t_k)} \qquad (7)$$

with

$$r(t)=\frac{a^2b(t-x_1)}{[(t-x_1)^2+a^2]^2}+\frac{c^2d(t-x_2)}{[(t-x_2)^2+c^2]^2}$$

In equation (7), $Z_j'(t_j)$ are determined by the numerical conformal mapping method [7].

Analytical expressions for the gravitational stresses in the ridges and valleys with the geometry of Figures 1a and 1b can be obtained by substituting equations (1)-(7) for equations (24)-(29) in [12]. All the other equations in Pan *et al.* [12] remain the same.

NUMERICAL EXAMPLES

The rock mass in Figures 1a and 1b is assumed to be transversely isotropic with planes of transverse isotropy parallel to the z axis and dipping at an angle ψ toward the +x axis. For that special orientation, it was shown by Pan *et al.* [12] that the rock mass deforms under a condition of plane strain in the x,y plane. Furthermore, at each point in the rock mass two of the three principal gravitational stresses are located in the x,y plane and the longitudinal stress σ_{zz} is the third principal stress. At each point in the rock mass, the dimensionless stress ratios $\sigma_{xx}/\rho g|d|$, $\sigma_{yy}/\rho g|d|$, $\sigma_{xy}/\rho g|d|$ and $\sigma_{zz}/\rho g|d|$ depend on four ratios of elastic constants: E/E', G/G', ν and ν' where (i) E and E' are Young's moduli in the plane of transverse isotropy and in direction normal to it, respectively, (ii) ν and ν' are Poisson's ratios characterizing the lateral strain response in the plane of transverse isotropy to a stress acting parallel or normal to it, respectively, (iii) G' is the shear modulus in planes normal to the plane of transverse isotropy, and (iv) $G=0.5\,E/(1+\nu)$ is the shear modulus in the plane of transverse isotropy. The stress ratios also depend on the dip angle, ψ, of the planes of transverse isotropy, the coordinates $(x/|d|,\ y/|d|)$ of the points at which the stresses are calculated and the ratios $a/|d|$, $b/|d|$, $c/|d|$, $d/|d|$, $x_1/|d|$ and $x_2/|d|$ describing the geometry of the asymmetric ridge or valley.

In the following numerical examples, the stress results are presented using trajectories and contours of dimensionless principal stresses $\sigma_1/\rho g|d|$ and $\sigma_2/\rho g|d|$ where σ_1 and σ_2 are the maximum and minimum in-plane principal stresses in the x,y plane normal to the ridge or valley axis. The variations of those two stress components along the ground surface is also discussed.

Figures 2a and 2b show the principal stress trajectories for the asymmetric ridge and valley of Figures 1a and 1b, respectively. The rock mass elastic constants are fixed with $E/E'=G/G'=3$, $\nu=0.25$, and $\nu'=0.15$. The dip angle, ψ, of the planes of transverse isotropy is equal to 0°. The principal stresses are oriented parallel and normal to the ground surface along the boundary of the ridge and valley and gradually turn to become horizontal and vertical with depth. Compression is dominant in the ridge of Figure 2a and tensile stresses $\sigma_2/\rho g|d|$ develop near the surface of the valley of Figure 2b. Finally, Figures 2a and 2b indicate that compared to the isolated and symmetric ridges and valleys discussed in Pan *et al.* [12], the gravitational stress field is no longer symmetric when ψ is equal to 0°. Other analysis conducted with the geometry of Figures 1a and 1b has shown that the magnitudes of $\sigma_1/\rho g|d|$ along the boundary of the ridge and $\sigma_2/\rho g|d|$ along the boundary of the valley decrease with increasing dip angle, ψ, and that the extent of the tensile region depends on the value of the dip angle. Also, it was found that the principal stresses adjust to the horizontal and vertical directions more rapidly with depth for vertically anisotropic rock masses ($\psi=90°$) than for rock masses with horizontal anisotropy ($\psi=0°$).

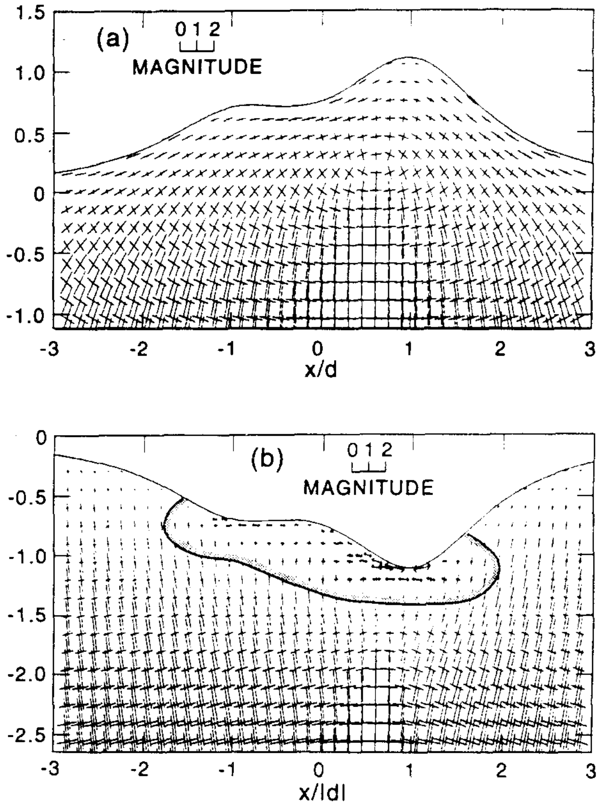

Figure 2. Trajectories of principal stresses $\sigma_1/\rho g|d|$ and $\sigma_2/\rho g|d|$ for the asymmetric ridge (a) and valley (b) of Figures 1a and 1b. Rock mass has horizontal planes of transverse isotropy with $E/E'=G/G'=3$, $\nu=0.25$, $\nu'=0.15$. The shaded region in (b) represents the tensile zone near the valley surface.

Figure 3a shows the contours of maximum principal stress $\sigma_1/\rho g|d|$ for the ridge of Figure 1a and for a rock mass with $E/E'=1$, $G/G'=3$, $\nu=0.25$, $\nu'=0.15$ and $\psi=90°$. Figure 3b shows the variation of $\sigma_1/\rho g|d|$ along the ground surface for E/E' = 1, 2 and 3. We note from Figure 3a that near the ground surface, the distribution of $\sigma_1/\rho g|d|$ is complicated with local maxima and minima. As shown in Figure 3b, the location of those extrema is controlled by the surface topography and their magnitude decreases as E/E' increases.

Figures 4a shows the contours of minimum principal stress $\sigma_2/\rho g|d|$ for the valley of Figure 1b and for a rock mass with $E/E'=G/G'=3$, $\nu=0.25$, $\nu'=0.15$ and $\psi=45°$.

Figure 4b shows the variation of $\sigma_2/\rho g|d|$ along the ground surface for ν' equal to 0.15, 0.25 and 0.35. It appears that less tension develops in the valleys walls as ν' increases.

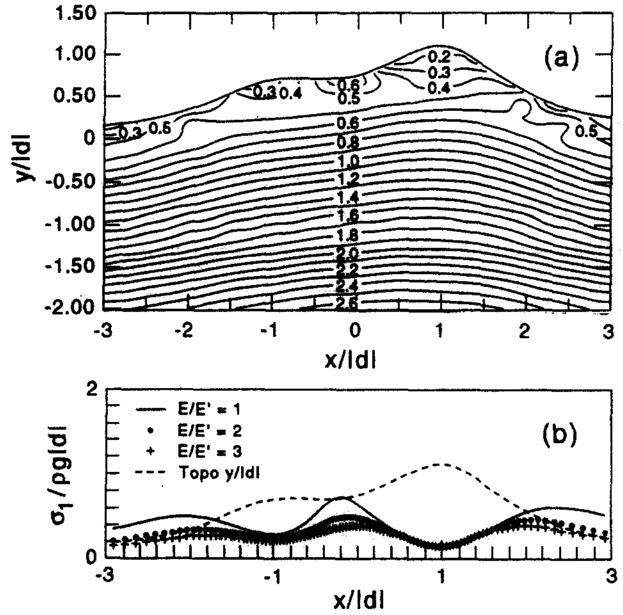

Figure 3. (a) Contours of $\sigma_1/\rho g|d|$ for the ridge of Figure 1a with ψ=90°, E/E'=1, G/G'=3, ν=0.25 and ν'=0.15. (b) Variation of $\sigma_1/\rho g|d|$ along the ground surface.

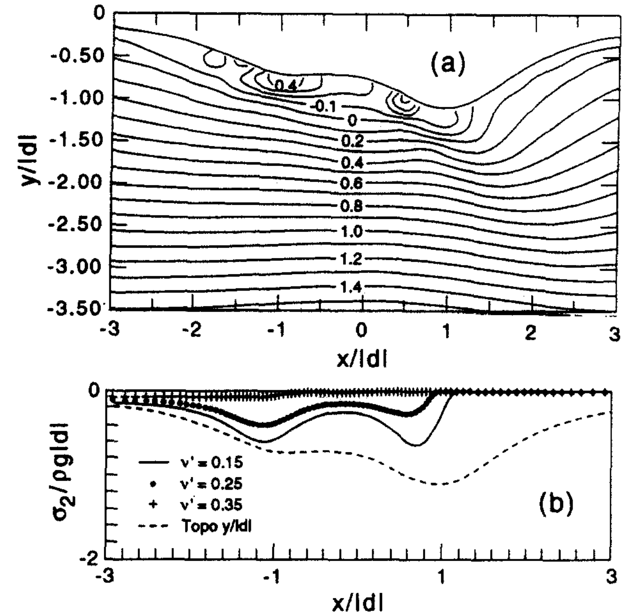

Figure 4. (a) Contours of $\sigma_2/\rho g|d|$ for the valley of Figure 1b with ψ=45°, E/E'=G/G'=3, ν=0.25 and ν'=0.15. (b) Variation of $\sigma_2/\rho g|d|$ along the ground surface.

CONCLUSION

The method proposed by Pan and Amadei [7] can be used to predict analytically the distribution and magnitude of gravitational stresses in long asymmetric ridges and valleys with complex topography. The latter is obtained by superposition of the topographies of symmetric ridges and valleys. The magnitude and distribution of gravitational stresses in ridges and valleys depend on several parameters such as (1) the ridge and valley geometry, (2) the orientation of the anisotropy with respect to the ridge and valley axis and (3) the degree of rock anisotropy defined by ratios of elastic constants such as E/E', G/G', ν and ν' for transversely isotropic rocks. For rock masses with planes of anisotropy that are parallel to the valley or ridge axis, two of the three principal stresses are in the plane normal to the valley or ridge axis and the longitudinal stress is the third principal stress.

In the examples presented in this paper, it is shown that when the ground surface is not horizontal, the principal stresses are no longer horizontal and vertical. At the ground surface, they are parallel and perpendicular to the topography (in the absence of surface loads). Then, they gradually turn to become horizontal and vertical with depth. As shown in this paper, there can be several maxima and minima of compressive stresses near the surface of asymmetric ridges and tensile stresses near the surface of asymmetric valleys.

Acknowledgment--This research is funded by National Science Foundation, Grant MS-9215397.

REFERENCES

1. Savage W.Z., Swolfs H.S and Powers P.S. Gravitational stresses in long symmetric ridges and valleys. *Int. J. Rock Mech. Min. Sci. & Geomech. Abstr.* **22**, 291-302 (1985).
2. Savage W.Z. and Swolfs H.S. Tectonic and gravitational stress in long symmetric ridges and valleys. *J. Geophys. Res.* **91**, 3677-3685 (1986).
3. McTigue D.F. and Mei C.C. Gravity induced stresses near topography of small slopes, *J. Geophys. Res.* **86**, 9268-9278 (1981).
4. McTigue D.F. and Mei C.C. Gravity induced stresses near axisymmetric topography of small slopes, *Int. J. Num. & Anal. Meth. in Geomech.* **11**, 257-268 (1987).
5. Liu L. and Zoback M.D. The effect of topography on the state of stress in the crust: Application to the site of the Cajon Pass Scientific Drilling Project, *J. Geophys. Res.* **97**, 5095-5108 (1992).
6. Liao J.J., Savage W.Z. and Amadei B. Gravitational stresses in anisotropic ridges and valleys with small slopes, *J. Geophys. Res.* **97**, 3325-3336 (1992).
7. Pan E. and Amadei B. Stresses in an anisotropic rock mass with irregular topography, accepted for publication in *ASCE Jnl. of Eng. Mech.* (1993).
8. Amadei B. and Pan E. Gravitational stresses in anisotropic rock masses with inclined strata, *Int. J. Rock Mech. Min. Sci. & Geomech. Abstr.* **29**, 225-236 (1992).
9. Lekhnitskii S. G. *Theory of Elasticity of an Anisotropic Elastic Body*. Holden-Day, San Francisco (1963).
10. Trummer M. R. An efficient implementation of a conformal mapping method based on the Szegö kernel. *SIAM J. Numer. Anal.* **23**, 853-872 (1986).
11. Muskhelishvili N. I. *Singular Integral Equations*. Noordhoff, Groningen, The Netherlands (1972).
12. Pan E., Amadei B. and Savage W. Z. Gravitational stresses in long symmetric and anisotropic ridges and valleys. Submitted to *Int. J. Rock Mech. Min. Sci. & Geomech. Abstr.*